Bioorganic & Medicinal Chemistry 17 (2009) 919–928

Contents lists available at ScienceDirect

Bioorganic & Medicinal Chemistry

journal homepage: www.elsevier.com/locate/bmc

Spectroscopic and calorimetric studies on the DNA recognition of pyrrolo[2,1-*c*][1,4]benzodiazepine hybrids

Michael Rettig [a], Ahmed Kamal [b], R. Ramu [b], Judith Mikolajczak [a], Klaus Weisz [a,*]

[a] *Institut für Biochemie, Ernst-Moritz-Arndt-Universität Greifswald, Felix-Hausdorff-Str. 4, D-17487 Greifswald, Germany*
[b] *Division of Organic Chemistry, Indian Institute of Chemical Technology, Hyderabad 500007, India*

ARTICLE INFO

Article history:
Received 18 June 2008
Revised 17 October 2008
Accepted 12 November 2008
Available online 19 November 2008

Keywords:
Calorimetry
DNA recognition
Pyrrolobenzodiazepine
Spectroscopy

ABSTRACT

DNA binding of two hybrid ligands composed of an alkylating pyrrolo[2,1-*c*][1,4]benzodiazepine (PBD) moiety tethered to either a naphthalimide or a phenyl benzimidazole chromophore was studied by DNA melting experiments, UV and fluorescence titrations, CD spectroscopy and isothermal titration calorimetry (ITC). Binding of both hybrids results in a remarkable thermal stabilization with an increase of DNA melting temperatures by up to 40 °C for duplexes that allow for a covalent attachment of the PBD moiety to guanine bases in their minor groove. CD spectroscopic measurements suggest that the naphthalimide moiety of the drug interacts through intercalation. In contrast, the PBD-benzimidazole hybrid binds in the DNA minor groove with a preference for $(A,T)_4G$ sequences. Whereas the binding of both ligands is enthalpy-driven and associated with a negative entropy, the benzimidazole hybrid exhibits a less favourable binding enthalpy that is counterbalanced by a more favourable entropic term when compared to the naphthalimide hybrid.

1. Introduction

Genomic DNA is targeted by many natural and synthetic low molecular weight compounds that upon binding to double-stranded nucleic acids through alkylation, intercalation and minor or major groove binding may interfere with various biological processes. In addition to the direct manipulation of genomic sequences due to their specific chemical reactivity, such drugs may also act as artificial regulators of gene expression through interfering with the binding of transcription factors or enzymes that regulate DNA topology such as topoisomerases I and II. Thus, the pyrrolo[2,1-*c*][1,4]benzodiazepine (PBD) drugs anthramycin, tomaymycin or DC-81 belong to a family of potent tricyclic anticancer antibiotics, that are isolated from various *Streptomyces* species and that bind to the minor groove of double-stranded DNA forming a covalent bond to the exocyclic amino group of a central guanine within a three base pair recognition site (Fig. 1).[1–3] In contrast, 1,8-naphthalimide-based antitumor drugs like amonafide exhibit a topoisomerase II inhibitory activity forming complexes with DNA through intercalation.[4,5] Similarly, the bis-benzimidazole Hoechst 33258 has been shown to inhibit DNA topoisomerase I, binding preferentially in the DNA minor groove at stretches consisting of 3–4 consecutive A/T base pairs.[6,7]

Potential applications of these drugs in diagnosis, molecular biology and medicine critically depend on the selective binding to a defined sequence of DNA. For targeting double-helical DNA with sufficient selectivity, DNA binding drugs should preferably recognize a target sequence of about ten base pairs in length and bind to it with high affinity. However, due to their size limitations many of the small DNA binding ligands are only capable of recognizing a very limited stretch of duplex DNA and the resulting poor sequence selectivity mostly limits their practical utility. As a consequence, much effort has been devoted to the development of DNA binding drugs with enhanced binding selectivity and affinity over the past years. For increasing the type of drug–DNA interactions, a variety of ligands with an extended string of repeating binding motifs were designed and often found to exhibit superior affinity, sequence selectivity or reactivity when compared to the corresponding simple lead compounds. These include pyrrolobenzodiazepine dimers with interstrand cross-linking ability,[8,9] dimeric naphthalimides[10] and bis-benzimidazoles[11] as well as minor groove binding pyrrole–imidazole hairpin polyamides[12,13] originally derived from the smaller natural drugs netropsin and distamycin A. Structural variants of the latter are called lexitropsins whereas combilexins are composed of an oligoamide core linked to various intercalators to form hybrid molecules of structurally quite different DNA binding domains with intercalating and minor groove binding activity.[14]

Likewise, hybrid molecules bearing a pyrrolo[2,1-*c*][1,4]benzodiazepine moiety with alkylating activity and linked to different DNA binding structural units have recently been shown to be promising inhibitors of cancer cell growth with cytotoxicity in a number of cell lines.[15] Although an understanding of the forces

* Corresponding author. Tel.: +49 (0)3834 864426; fax: +49 (0)3834 864427.
E-mail address: weisz@uni-greifswald.de (K. Weisz).

0968-0896/$ - see front matter © 2008 Elsevier Ltd. All rights reserved.
doi:10.1016/j.bmc.2008.11.033

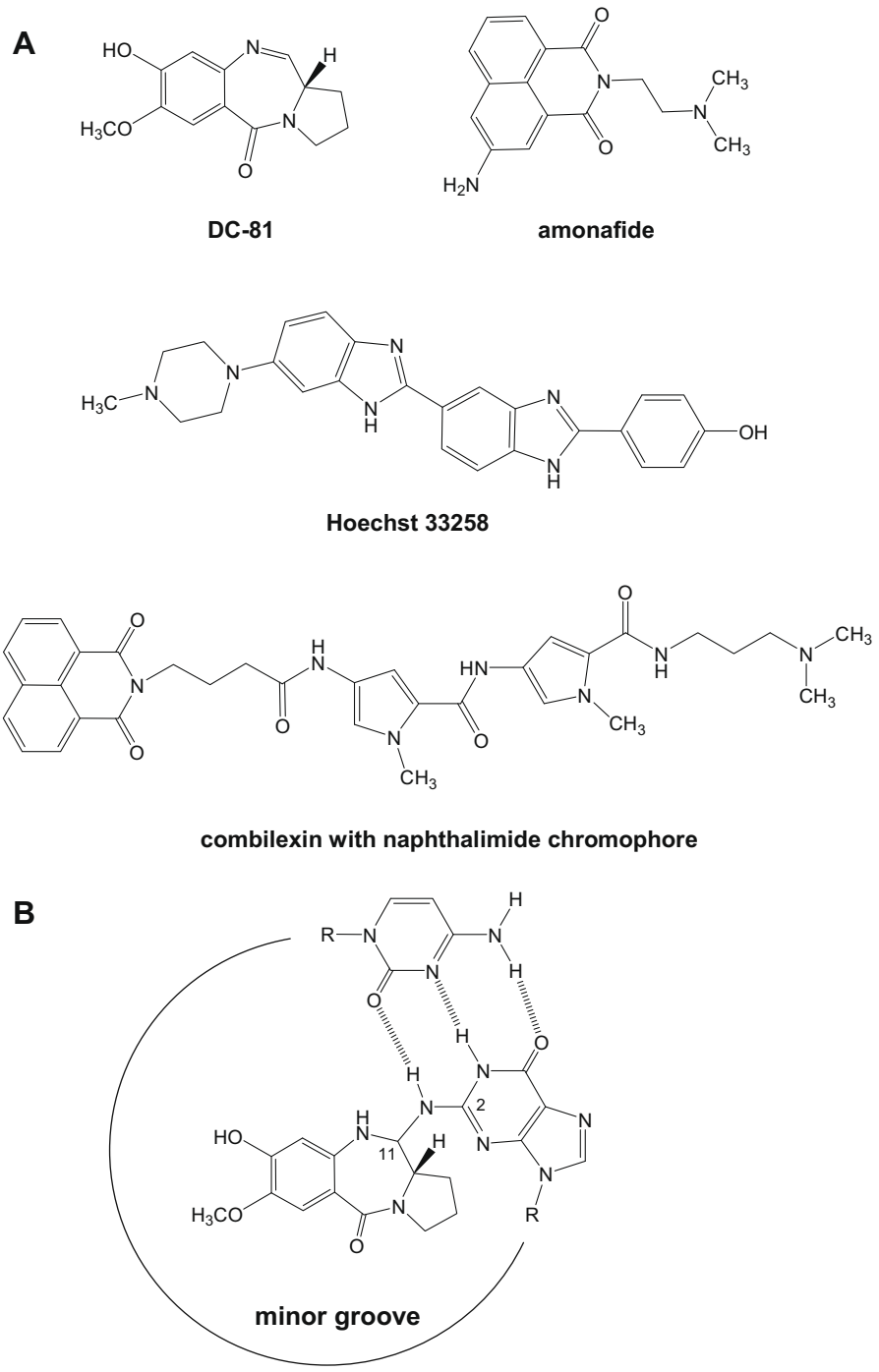

Figure 1. (A) Structures of DC-81, amonafide, Hoechst 33258 and a combilexin. (B) Covalent adduct of DC-81 with DNA from C11 of the PBD to the guanine 2-amino group of a CG base pair.

responsible for the affinity and selectivity toward a DNA duplex is crucial for future rational drug design, specific binding interactions of those hybrids have not been scrutinized so far. Here we report on the first detailed study of the sequence selectivity and binding thermodynamics of two pyrrolo[2,1-*c*][1,4]benzodiazepine drugs. Hybrid **1** is composed of a PBD moiety tethered to a coplanar naphthalimide DNA binding motif[16,17] with a potential propensity for intercalation. In contrast, the PBD unit of hybrid **2** is covalently linked to a 2-phenyl-benzimidazole motif[18] derived from the bis-benzimidazole minor groove binder Hoechst 33258 (Fig. 2). Because a piperazine ring has previously been shown to impart a large favorable binding interaction for minor groove recognition,[19,20] it has been introduced as part of the linker in **1** or through attachment to the benzimidazole terminus in **2**.

2. Results

2.1. UV melting experiments

To study the affinity and sequence selectivity of binding for the ligands **1** and **2**, 11 different duplexes composed of self-complementary and non-self-complementary 10mer oligonucleotides

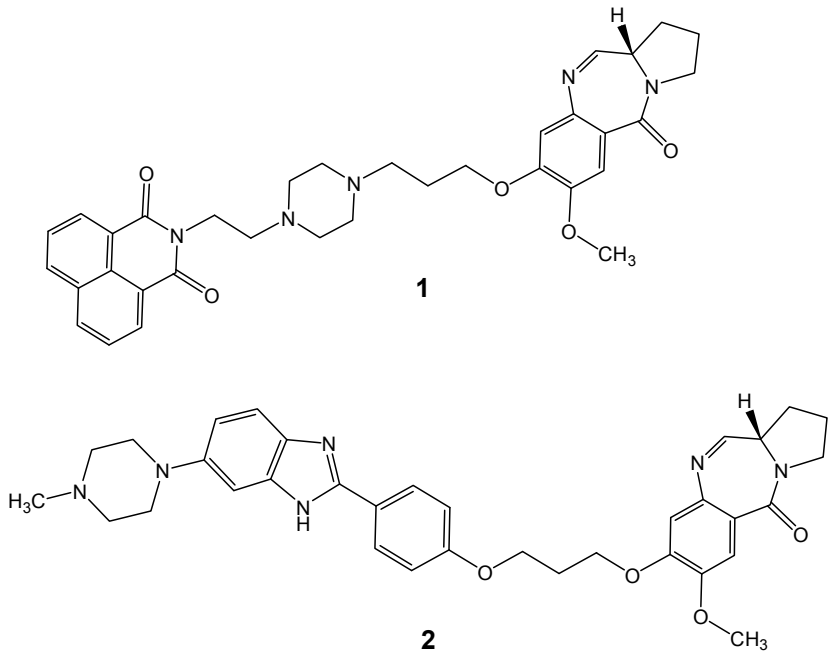

Figure 2. Structures of pyrrolobenzodiazepine hybrids **1** and **2**.

were used as targets for the drugs. The duplex sequences and the results of the UV melting experiments are summarized in Table 1.

In general, the duplex-to-single strand transition is characterized by a single cooperative absorbance change as a function of temperature. Drug binding to the duplex is expected to enhance its stability when compared to single strands and an increase in the duplex melting temperature upon drug addition is therefore associated with its relative binding affinity. Except for the all-AT duplex **D1**, sequences were designed to have a central tract of 2–4 AT base pairs of varying sequences flanked on either side by a GC base pair. In **D2b** and **D2c**, one or both GC base pairs have additionally been replaced by IC base pairs lacking an exocyclic 2-amino substituent on the inosine.

Table 1
UV melting temperatures T_m (°C) for the oligonucleotide duplexes without and with addition of **1** and **2** in a 2:1 drug:duplex molar ratio[a].

Duplex		T_m w/o drug	T_m w. **1**	ΔT_m **1**	T_m w. **2**	ΔT_m **2**
D1	5′-A A T A T A T A T T 3′-T T A T A T A T A A	13	22	9	23	10
D2a	5′-A A C A T A T G T T 3′-T T G T A T A C A A	29	63	34	62	33
D2b	5′-A A I A T A T G T T 3′-T T C T A T A C A A	21	55.3	34.3	60	39
D2c	5′-A A C A T A T I T T 3′-T T I T A T A C A A	13	19.5	6.5	22	9
D2e	5′-A A T A T A T G T T 3′-T T A T A T A C A A	20.5	55.5	35	57.5	37
D3	5′-A T C T A T A G A T 3′-T A G A T A T C T A	19	58.5	39.5	—[b]	—[b]
D4	5′- A A C A T T A G T T 3′- T T G T A A T C A A	25.5	62.3	36.8	59.8	34.3
D5	5′- A A C A A T T G T T 3′- T T G T T A A C A A	33.5	63.8	30.3	66	32.5
D6	5′- A T C A T T A G A T 3′- T A G T A A T C T A	24.5	62.2	37.3	59.0	34.5
D7	5′- A A C C T A T G T T 3′- T T G G A T A C A A	31	62.5	31.5	58.5	27
D8	5′- A A C C T A G G T T 3′- T T G G A T C C A A	35	70	35	35	0

[a] Average of 3–4 determinations.
[b] Not determined due to non-cooperative melting.

Typical thermal denaturation profiles for the drug–DNA mixtures are shown in Figure 3. The melting temperature of 13 °C for **D2c** increases by 6.5–19.5 °C upon adding **1** in excess of double-stranded DNA. As shown in Figure 3(top), no significant hysteresis effects are observed for corresponding heating and cooling cycles in agreement with reversible drug binding and fast dynamic equilibria. Likewise, melting experiments with the all-AT duplex **D1** exhibit a modest increase in the melting temperature of 9 °C upon addition of ligand **1**, again exhibiting a fully reversible melting profile. A similar increase in duplex thermal stabilization of these sequences is also observed for hybrid **2**.

A very different behaviour in melting is seen after addition of both ligands to the duplexes containing a guanine base. A representative example is shown in Figure 3(bottom) for the **D2b** duplex in the presence of excess **1**. A monophasic transition at high temperatures is observed in the first heating profile after equilibration of the mixture for several days. This transition which has to be attributed to the formation of a drug–DNA complex is considerably shifted compared to the melting transition of the free oligonucleotide duplex by about 34 °C and 39 °C for **1** and **2**, respectively. In contrast, the nucleic acid shows only a low-temperature transition with a transition temperature corresponding to the melting of drug-free duplex upon cooling. Also, absorbances after cooling have somewhat increased when compared to absorbances measured at the start of the first heating cycle. Interestingly, both the low- and high-temperature transition appear in a second subsequent heating ramp, however, the low-temperature transition can be reduced or eliminated again after equilibration for a prolonged period of time (not shown). Taken together, very slow kinetics in drug binding and cleavage of the labile covalent adduct after strand dissociation, as observed for other PBD derivatives,[1,21,22] must be responsible for such non-reversible behavior seen in these melting profiles. It has to be noted, that transition temperatures are not affected by the drug-to-DNA molar ratio, supporting the existence of only one defined complex in equilibrium with the free duplex. Also, replacing one of the two GC base pairs by an IC base pair in duplex **D2a** does not compromise the thermal stabilization of bound drug and even results in an enhanced stability of complexes with **2**, suggesting the covalent

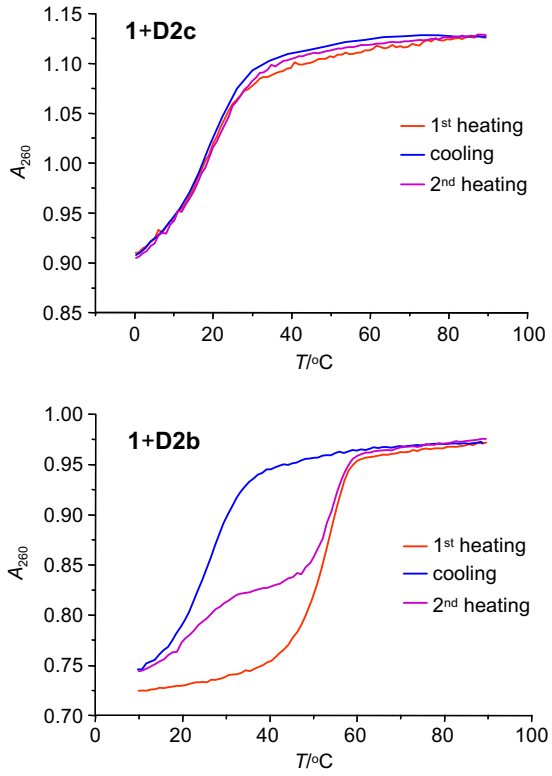

Figure 3. UV melting profiles for drug-duplex mixtures (2:1 molar ratio) in BPS buffer. For experimental conditions see text.

attachment of one hybrid molecule in either duplex. In contrast, with both guanine bases replaced by inosine to disable covalent adduct formation, increases in duplex melting temperatures drop down dramatically upon addition of both hybrids to <10 °C. Compared to the significant effects on duplex stabilization of the two PBD hybrids, the non-conjugated PBD drug DC-81 used as a reference does not result in a noticeable duplex thermal stabilization upon addition to duplex **D2a** as well as to guanine-free **D2c** under identical conditions (data not shown).

The increase in melting temperatures after addition of either **1** or **2** amounts to >30 °C for duplexes with a central $(A,T)_4G$ sequence. One of the largest thermal stabilization on duplexes reported under such conditions so far is observed for complexes **D3**·**1** and **D2b**·**2** with TATAG and ATATG tracts, exhibiting a temperature for the duplex half-dissociation raised by nearly 40 °C. No melting temperature could be determined for **D3** in the presence of **2** due to non-sigmoidal melting curves. The reason for such atypical behaviour remains unknown but may be attributed to the coexistence of several complexes with unspecific drug binding.

Binding affinities as judged from the ΔT_m values of >30 °C are not significantly compromised for the naphthalimide hybrid **1** upon shortening the central AT tract to three and two AT base pairs in **D7** and **D8**, respectively. However, the benzimidazole hybrid **2** shows a noticeable decrease in thermal stabilization with the target duplex **D7** and fails to bind **D8** with only two centrally located AT base pairs.

2.2. CD spectroscopy

The free ligands exhibit small Cotton effects below 300 nm because of the intrinsic asymmetry of the PBD ring system with its single chiral center. Since the naphthalimide moiety itself is not optically active, no Cotton effect is observed at its absorption wavelength at 342 nm. Figure 4(top) shows the CD spectra of free drug **1**, the sum of spectra for free **D2a** and drug as well as of a mixture of **D2a** and **1**. When compared to the sum of CD spectra for free **D2a** and **1**, the CD spectrum of the drug–DNA mixture has changed. The strong negative and positive bands observed at around 250 and 270 nm, indicative of a B-type duplex structure, are slightly shifted to shorter wavelengths on complex formation with an increase in amplitude for the positive band. The two weak negative long-wavelength bands, centered at 295 nm and 342 nm and only observed for the drug–DNA mixture, must arise from bound drug. The CD band at 342 nm must be attributed to an induced CD effect of the naphthalimide chromophore upon binding to DNA. Interestingly, the additional negative CD band at 295 nm is only observed in guanine-containing duplexes and hence may be associated with the formation of the covalent bond between the PBD and a guanine amino group.

As shown in Figure 4(bottom), significant changes of the CD spectrum are also associated with binding of the benzimidazole hybrid **2** to the **D2a** duplex. Again, a shift towards shorter wavelengths for both the strong negative and positive bands at around 250 and 270 nm is observed after addition of the drug to the duplex. This is accompanied by a significant increase in signal amplitude of the positive band and a moderate decrease in amplitude of the short-wavelength negative band. In addition to the negative CD band at 295 nm also observed for the binding of **1**, a positive band centered at 315 nm is observed after addition of hybrid **2** to the duplex and results from an induced Cotton effect of the benzimidazole chromophore.

2.3. UV titration

Because the drug should bind in the duplex minor groove prior to the formation of a covalent bond to the guanine amino group

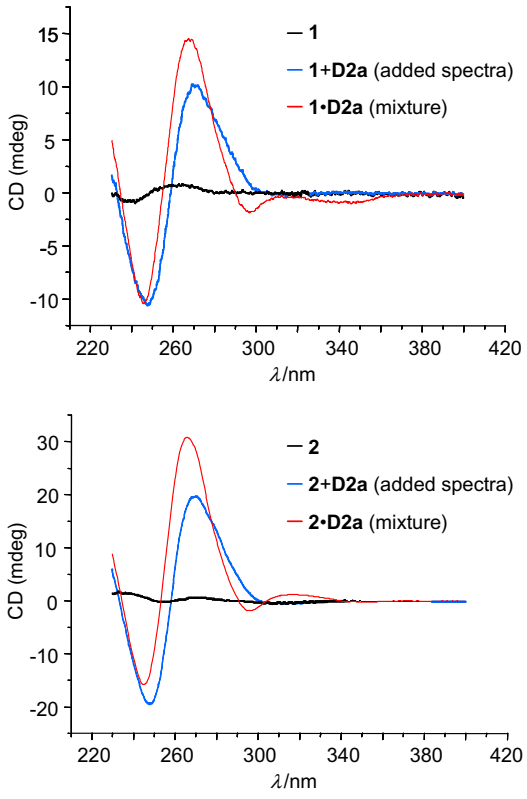

Figure 4. Circular dichroism spectra showing the influence of binding on hybrids **1**, **2** and duplex **D2a** in BPS buffer.

located at its floor and in order to separate non-covalent binding interactions from additional covalent aminal bond formation with its slow kinetics (vide supra), guanines in duplex **D2a** were replaced by inosines for the following titration experiments. Also, by using the intramolecular hairpin duplex **D2d** (see Fig. 5), the double-helical structure exhibiting a melting temperature of 48 °C was significantly stabilized to enable measurements at 20 °C without any noticeable thermally induced duplex melting.

Upon addition of hairpin duplex **D2d** to a buffered solution of **1** and **2**, a decrease in the intensity of the long-wavelength absorption band with a hypochromicity of about 25% and 11% was observed, respectively. By comparison with the nearly identical absorption band found previously for a simple *N*-pyridiniumethyl-substituted naphthalene imide, the long-wavelength absorption of **1** at 342 nm can be assigned to electronic transitions of the naphthalimide moiety.[23] Likewise, the absorption band of **2** with its maximum at 319 nm must largely arise from the 2-phenylbenzimidazole structural unit. Whereas binding of **1** only results in a negligible wavelength shift of its absorption maximum, binding of **2** is accompanied by a bathochromic shift of 5 nm. More importantly, however, there is a single clean isosbestic point for **1** at 365 nm for all drug-to-duplex ratios indicating the presence of only one spectrally distinct drug–DNA complex in equilibrium with the free drug. Likewise, the absorption spectra of **2** indicate one major binding mode, however, small variations in the positioning of non-covalently bound drug may be responsible for the slightly blurred isosbestic point at 329 nm.

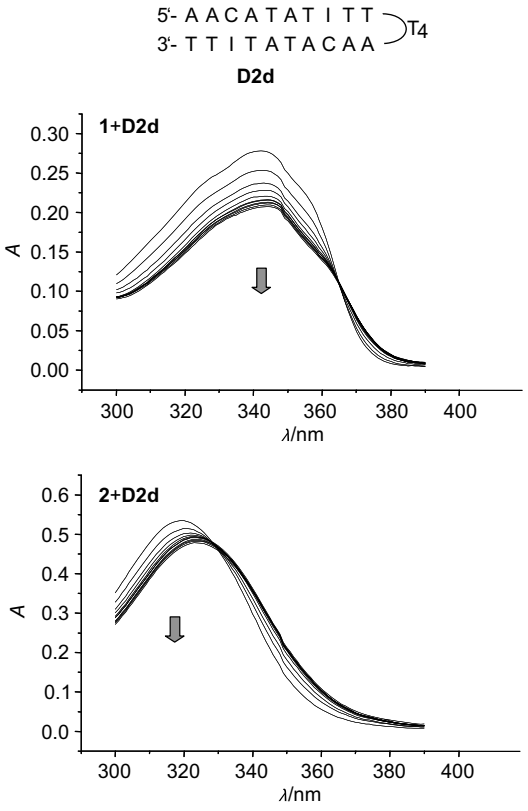

Figure 5. Absorption spectral changes observed upon addition of the hairpin duplex **D2d** (0–50 μM) to **1** (26 μM, top) and **2** (26 μM, bottom) in BPS buffer with 2% DMSO; arrows indicate the development of the absorption bands upon DNA duplex titration.

2.4. Fluorescence titration

The binding constant of the ligand to DNA was determined by titrating the drug solution with a concentrated solution of hairpin duplex **D2d** at 20 °C. A moderate decrease and significant increase in the drug fluorescence emission was observed during the addition of the duplex to hybrid **1** and **2**, respectively, resulting in the binding isotherms shown in Figure 6. The analysis of the spectroscopic titration curve is based on its fitting with an appropriate binding model [for an overview see (24)]. Structural considerations together with the UV spectroscopic data clearly support a major or even exclusive complex with a specific bimolecular drug–DNA association. Accordingly, by employing a 1:1 binding model a good overall fit to the fluorescence data was obtained as shown in Figure 6. For the non-covalent binding of the ligands, association constants of similar magnitude were determined from the titration data of **1** and **2.** These amount to $K_a = 3.8 \cdot 10^6\ M^{-1}$ for **1** and $K_a = 5.6 \cdot 10^6\ M^{-1}$ for **2** at 20 °C.

2.5. Isothermal titration calorimetry

Isothermal titration calorimetry was used to quantify the thermodynamics of non-covalent drug binding to duplex **D2d**. Figure 7 shows primary data for the titration of the hairpin duplex into a buffer solution of **1** and **2**. Such a reverse titration circumvents problems associated with the limited solubility of drug in aqueous buffer. Each peak in the upper panel corresponds to the heat released on addition of an aliquot of duplex to the drug. These data must be corrected for the dilution heats associated with the addition of DNA into buffer and buffer into drug solution. The heat of dilution for the latter was shown to be negligible. In contrast, titration of the DNA into aqueous buffer was found to be endothermic. Integration with respect to time after correcting for these dilution effects and normalization per mole of added duplex gives the corresponding binding isotherms (lower panel).

As shown in Figure 7, application of a simple independent binding site model (vide supra) for the interactions of ligands **1** and **2** with the hairpin structure leads to an excellent fit of the binding isotherm yielding the binding enthalpies ΔH° and equilibrium binding constants K_a. Additionally, the entropy and free energy of association ΔS° and ΔG° can be calculated from the other parameters according to the standard thermodynamic relationship $\Delta G^\circ = \Delta H^\circ - T\Delta S^\circ$. All parameters determined from ITC are summarized in Table 2.

Complex formation through drug binding is exothermic and in both cases counterbalanced by an entropy penalty. However, enthalpic and entropic contributions to the binding free energy differ between the two PBD hybrids. Thus, a more negative ΔH° for the binding of **1** is accompanied by a more unfavourable negative binding entropy ΔS°. As a result of this balancing effect, both drugs exhibit a moderately strong non-covalent binding with about the same overall free energy of association $\Delta G^\circ \sim -8.0$ kcal mol^{-1}. Note, that although smaller in magnitude by a factor of 5–6, association constants determined for the two hybrids by ITC show a reasonable agreement with the corresponding fluorescence titration data.

3. Discussion

3.1. Kinetics of binding

Covalent DNA adduct formation with various PBD drugs through alkylation of the guanine amino group in the DNA minor groove has previously been found to proceed with slow rates and to also depend on the hydrogen ion concentration.[21,25,26] Likewise, looking at the UV melting curves it becomes obvious, that the

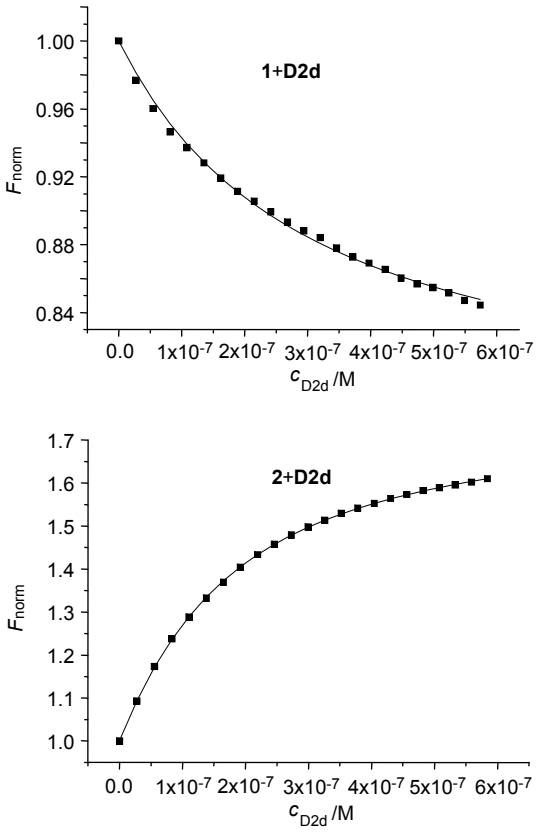

Figure 6. Fluorescence binding isotherms for **1** (top) and **2** (bottom) with hairpin duplex **D2d** at 20 °C. The concentration of the PBD-hybrid **1** and **2** was 20 nM and 67 nM, respectively. A fit to the data was carried out using a non-linear least-squares analysis as described in Section 5.

kinetics of covalent bond formation with the PBD hybrids is slow enough to require an extensive period of time for completion. This is reflected by the presence of a free duplex melting even with drug in excess and non-superimposable melting curves taken at different times. Thus, an increase in the ratio of hyperchromicities upon melting of the free and ligand-bound duplex is often observed for a second consecutive melting profile with only a short intervening period of equilibration. Likewise, after equilibration for several hours or days the amount of complex as estimated from hyperchromicities of the biphasic melting profile increased considerably in some cases. Alkylation of guanine-containing duplexes is also supported by TLC and HPLC analyses for these sequences, that clearly indicate the presence of some single-stranded DNA–drug adduct even under denaturing conditions (not shown). In contrast, only free DNA and free drug can be detected for duplexes lacking a guanine for covalent attachment. For the latter, only a monophasic time-independent melting profile was observed in the presence of drug in line with a fast equilibrium of free and non-covalently bound drug.

The aminal bond formed between the drug and the guanine 2-amino group is known to be labile and amenable to hydrolysis at acidic but also neutral pH when present on a single-stranded DNA, resulting in the liberation of free reactive drug upon thermal denaturation of the duplex.[27] The disappearance of a high-temperature transition in the cooling curves of GC containing sequences, leaving only the low-temperature transition attributed to the annealing of free oligonucleotide, clearly indicates significant hydrolysis occurring after duplex denaturation. However, a small increase in absorbance, as observed for some oligonucleotides after cooling below their melting temperature, may be attributed to a small fraction of single-stranded DNA–drug adduct whose hybridization with a complementary oligonucleotide is hampered for steric reasons.

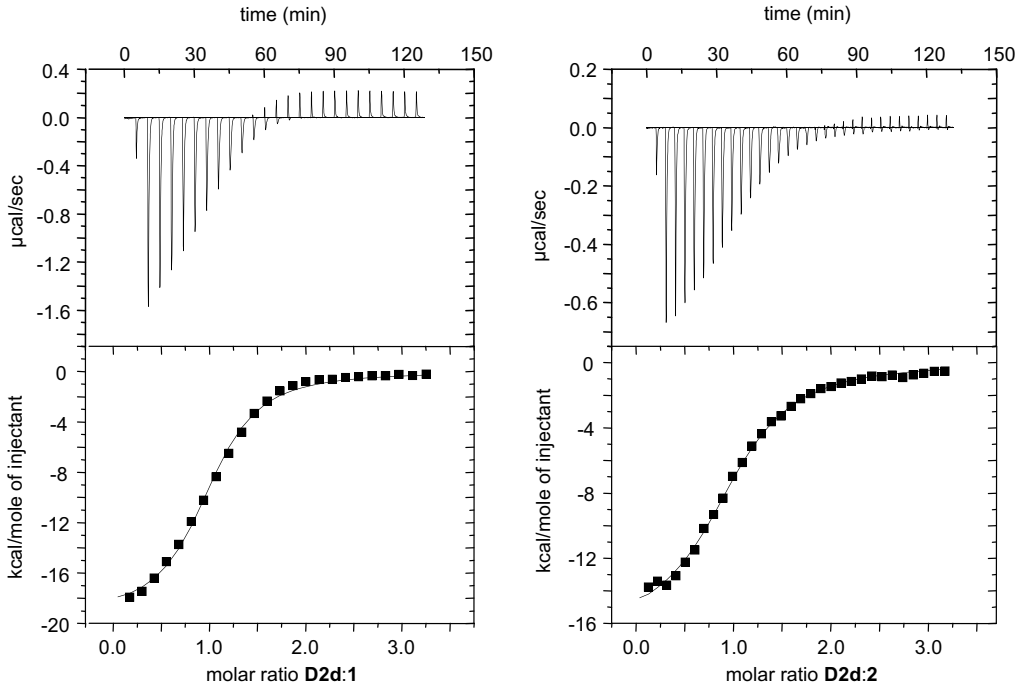

Figure 7. Calorimetric data for the titration of **1** (left) and **2** (right) with hairpin duplex **D2d** at 20 °C showing exothermic binding. ITC raw data give the power output for each 8-µL injection of titrant as a function of time and are presented in the top panel. The lower panel is obtained after peak integration and shows the heat produced per injection as a function of the duplex/ligand molar ratio (black squares) together with the best fit to the corrected binding isotherm (solid line). The initial drug concentration in the cell was 19 and 13 µM and the concentration of duplex titrant was 423 and 212 µM for the titration of **1** and **2**, respectively.

Table 2
Thermodynamic parameters for the binding of ligands **1** and **2** to hairpin duplex **D2d** at 20 °C

Ligand	K_a (M^{-1})	$\Delta H°$(kcal·mol^{-1})	$T\cdot\Delta S°$(kcal·mol^{-1})	$\Delta G°$(kcal·mol^{-1})
1[a]	$3.8\cdot10^6 \pm 0.4\cdot10^6$			−8.8
1[b]	$7.8\cdot10^5 \pm 3.9\cdot10^5$	−18.7 ± 2.2	−10.9 ± 2.5	−7.8
2[a]	$5.6\cdot10^6 \pm 2.0\cdot10^6$			−9.0
2[b]	$8.9\cdot10^5 \pm 4.4\cdot10^5$	−14.5 ± 2.2	−6.6 ± 2.4	−7.9

[a] Obtained from fluorescence titrations; values are given as averages from two independent experiments with standard deviations indicated.
[b] Obtained from ITC measurements; values are given as averages from three independent experiments with standard deviations indicated.

3.2. Sequence selectivity

Based on the UV melting data, both hybrid drugs significantly stabilize duplexes containing GC base pairs with an increase in melting temperature ranging from 30 °C to 39 °C upon binding. Clearly, such a dramatic stabilization must be attributed to covalent adduct formation at guanine sites and consequently, stabilization upon non-covalent drug binding for duplexes lacking GC base pairs is significantly reduced with ΔT_m values $\leqslant$10 °C. However, duplex stabilization as indicated by elevated temperatures for strand dissociation is also influenced by sequence effects of the GC-containing double strand. Whereas binding of **1** exhibits ΔT_m values $\geqslant$30 °C for all duplexes studied, the benzimidazole hybrid **2** shows a noticeable drop in its thermal stabilization for duplexes with a shortened AT base pair tract upstream the GC site. Thus, with only three AT base pairs in **D7**, ΔT_m decreases to 27 °C and there is a complete loss of duplex stabilization with no indication of any drug binding in the case of duplex **D8** which features only two contiguous AT pairs. Structural models of hybrid **2** positioned within the duplex minor groove suggest that excluding its terminal piperazine ring, the PBD-benzimidazole hybrid will span four base pairs upstream from the guanine site of covalent attachment in line with its maximum stabilizing effect in the presence of an $(A,T)_4G$ tract. Apparently, the phenyl-substituted benzimidazole motif preferentially binds in the intrinsically narrow minor groove of AT sequences, a feature generally observed for minor groove binding ligands including Hoechst 33258. Accompanied by unfavourable steric or electrostatic effects within the minor groove, GC base pairs seem to kinetically and/or thermodynamically hamper initial drug binding by non-covalent interactions, a prerequisite for the formation of a covalent bond between the PBD moiety and an adjacent exocyclic guanine amino group.

Based on the length of the linker that connects to the PBD moiety, the naphthalimide chromophore in **1** is expected to closely match the location of the benzimidazole unit in **2** when positioned in the duplex minor groove. Thus, the naphthalimide does not seem to favor AT base pairs over GC base pairs at its binding site supporting an intercalative mode of binding within the mixed hybrid. Such interactions correspond to the intercalative binding found for other mono- and bisnaphthalimide ligands and supported by the observed CD spectral features (vide infra).[10,28] It is also interesting to note, that replacing the non-alkylated CG base pair following the $(A,T)_4$ tract in **D2a** by an IC or TA base pair to give **D2b** and **D2e** has no marked effect on the thermal duplex stabilization by hydrid **1**, but leads to noticeable differences in the hybrid **2**-mediated stabilization in line with direct drug–DNA interactions close to this base pair site.

Simple pyrrolo[2,1-*c*][1,4]benzodiazepine drugs have been shown to prefer binding at 5′-PuGPu-3′ sequences with 5′-PyG-Py-3′ sequences to be the least preferred target sites.[29] For the interstrand cross-linking PBD dimer SJG-136, a 5′-PuGATCPy-3′ tract was found to be the preferred binding site and the preference for an adenosine next to guanosine was attributed to favorable hydrogen bond interactions between the two PBD units and the adenine bases.[22] Based on the UV melting of the various target duplexes, such a preference is not immediately apparent for the two PBD hybrids as can be inferred from the considerable drug-mediated stabilizations of the **D2** duplexes carrying a TGT sequence. Obviously, the moderate sequence selectivity exhibited by the PBD drug is further leveled off by the additional naphthalimide or benzimidazole moieties within the hybrid molecules. A discrimination between the different AT-rich sequences by the ligand is suggested from differences in ΔT_m by up to 10 °C depending on the particular sequence of the central $(A,T)_4$ tract. However, especially in the case of more subtle differences, there is no direct way to assess binding affinities from differences in melting temperatures when the temperature dependence of binding constants is not known for the different complexes. Nevertheless it is interesting to note, that upon complex formation with **1**, duplexes with the same central AT-tract like **D4**/**D6** and **D2a**/**D2b**/**D2e** exhibit about the same increase in melting temperature, allowing sequences to be ordered according to increasing ΔT_m as follows: ΔT_m(5′-TATAG-3′) > ΔT_m(5′-ATTAG-3′) > ΔT_m(5′-ATATG-3′) > ΔT_m(5′-AATTG-3′). In contrast, hybrid **2** shows no obvious trend for such $(A,T)_4$ sequence selectivity with respect to ΔT_m.

3.3. Mode of binding

Considering the length of the oligonucleotide duplexes and the size of the hybrid drugs one can expect that the duplex can physically only accommodate one drug molecule for specific binding and such a 1:1 interaction is corroborated by the available experimental observations. Also, UV melting and titration data showing a well-defined melting temperature for the drug adducts and the presence of isosbestic points over a wide range of ligand-to-DNA ratios are consistent with a single predominant or even exclusive complex geometry. Additional weaker binding, for example, through outer non-specific association cannot be rigorously excluded, yet if present do not exhibit any noticeable effect on the various experiments. The long-wavelength UV absorptions of **1** and **2** attributable to the naphthalimide and benzimidazole structural units are both reduced in intensity upon duplex addition. The rather large hypochromic effect observed for bound **1** amounts to 25% and contrasts with a hypochromicity of only 11% found for **2**. This indicates strong electronic interactions between π-electrons of **1** and DNA bases characteristic of intercalating compounds. It has to be noted, however, that hypochromicities of up to 60% have been reported for some simple naphthalimide derivatives upon DNA intercalation.[10,23]

CD spectra provide additional information on the hybrid binding to the double helix. Changes in the DNA absorption region between 200 and 300 nm upon drug addition and developing signals of an induced CD (ICD) at the drug absorption above 300 nm confirm drug–DNA interactions associated with some structural perturbations of the duplex. In general, the specific drug orientation within the complex may be deduced from the sign of the ICD signal; however, its evaluation requires information about the transition dipole moment for the corresponding electronic transition of the ligand and remains ambiguous in certain cases.[30,31] On the other hand, a negative ICD at 350–365 nm has also been found for a naphthalimide-pyrrole-carboxamide compound of the combilexin-type thought to bind through partial intercalation.[14] In contrast, a positive ICD similar to hybrid **2** between 300 and 400 nm has previously been reported for the bis-benzimidazole derivative Hoechst 33258 binding in the minor groove of a dodecamer duplex.[32,33]

3.4. Thermodynamics of binding

The determination of binding constants by spectroscopic or calorimetric titration experiments requires measurements on the system at thermodynamic equilibrium. To circumvent slow kinetics for the adduct formation with the PBD hybrids during titration, duplexes with guanines exchanged for inosine nucleosides were employed for a thermodynamic characterization of complex formation. This offers a detailed description of the non-covalent drug–DNA association that is expected to precede and guide any final covalent bond formation with a guanine amino group located at the floor of the duplex minor groove.

Binding constants determined by fluorescence and ITC experiments indicate moderately strong non-covalent drug–DNA interactions with values of $K_a \sim 10^6\ M^{-1}$. Surprisingly, given the very different non-PBD moieties of **1** and **2**, differences for the two hybrids in K_a are marginal. Association constants of 10^4–$10^5\ M^{-1}$ have previously been determined for the binding of simple naphthalimide derivatives to calf-thymus DNA[4,23] as well as for furonaphthalimides binding to double-helical DNA with an observed preference for GC-rich sequences.[10] On the other hand, association constants for **2** are considerably smaller by up to 2 orders of magnitude when compared to the high-affinity bis-benzimidazole minor groove binder Hoechst 33258.[19,33,34] In line with the absence of any significant thermal stabilization of duplexes in the presence of the free PBD drug DC-81, the PBD moiety of the hybrids is expected to be only a minor contributor to the overall binding within a non-covalent DNA complex but will greatly promote binding through covalent adduct formation at G-containing sequences.

Binding constants determined by spectroscopic and calorimetric methods often show significant differences due to inherent inaccuracies of the analysis. Thus, the evaluation of spectroscopic titration data is based on a binding reaction that follows a two-state transition between free and bound ligand molecules. In contrast, ITC only provides for reliable association constants if the product of K_a and the total concentration of titrate are in a range 1–1000. For tight binding with high K_a values, appropriate concentrations would be too low to produce a heat signal within the sensitivity range of the instrument and the requirement of higher concentrations will inevitably compromise the accuracy. For the present studies, association constants from both techniques are found to be within the same order of magnitude and translate to only a moderate difference in the binding free energy of about 1 kcal mol^{-1}, thereby gaining additional confidence in the proper analysis of the corresponding data. Indeed, moderately strong binding with $K_a \sim 10^6\ M^{-1}$ in the present system permits accurate determination of binding constants from ITC measurements employing concentrations in the 10^{-5} M range. On the other hand, the modest deviations in the binding constant as obtained from the fluorescence titration data may reflect a binding event that does not completely conform to a simple lock-and-key mechanism as can be anticipated by the structure of the hybrids with two drug moieties linked by a flexible spacer.

Isothermal titration calorimetry also provides for a direct determination of the molar binding enthalpy ΔH° for the non-covalent drug–DNA interaction. The sigmoidal binding isotherm obtained rules out the presence of multiple non-identical binding sites with different intrinsic affinities and again points to a 1:1 complex. Given the small temperature range available for additional fluorescence titration experiments, we did not attempt to also determine binding enthalpies by spectroscopy through a van't Hoff analysis of temperature dependent association constants.

Binding of both **1** and **2** to the duplex is enthalpically driven with a large negative ΔH°. The enthalpy change measured by ITC has major contributions from hydrogen bonding, van der Waals interactions and electrostatic interactions between ligand and DNA and also from reorganization of water molecules on complex formation whose influence on ΔH° is difficult to assess. On the other hand, unfavourable changes in entropy partly balance favourable binding enthalpies for the two drugs. The entropy is thought to be largely dominated by hydration or hydrophobic effects and a positive ΔS° as previously observed for some drugs is a strong indication, that the effect of water molecules expelled from the complex interface drives their binding to the DNA. In contrast, with two structural units connected by a flexible linker, a loss of rotational and translational degrees of freedom upon binding may significantly contribute to the substantial entropic penalty of complex formation for the two PBD hybrids.

As seen from Table 2 and shown in Figure 8, enthalpic and entropic contributions to the free energy of binding are noticeably different for the two PBD drugs. A more favourable negative enthalpy change for the naphthalimide hybrid is offset by a less favourable entropy of binding. A comparison of DNA binding drugs whose thermodynamics have been studied by direct calorimetric methods reveal, that for most intercalators like ethidium a large negative enthalpy term dominates the entropic term and constitutes the major contributor to the favourable free energy.[35–38] For minor groove recognition, thermodynamic profiles are in general strongly sequence dependent but in many cases show a favourable binding entropy due to significant hydrophobic interactions and release of bound water on binding. Thus, the endothermic binding of Hoechst 33258 to oligonucleotide duplexes is considered a rigid body interaction with little conformational changes to either DNA or drug and exclusively driven by hydrophobic effects.[34,36,37] The observed shift to a less favourable binding enthalpy but a more favourable binding entropy when substituting the phenyl benzimidazole for the naphthalimide moiety in the PBD hybrids is therefore compatible with a shift from a partially intercalative binding mode for **1** to an exclusive minor groove binding mode for **2**. Hydrophobic contributions to the binding free energy may be evaluated by the transfer free energies of ligands from the aqueous solution to the interior or minor groove of the DNA duplex. Heat capacity changes obtained from the temperature dependence of ΔH° and changes in the solvent-accessible surface area as determined from the three-dimensional structure of complexes have been linked and used to estimate the free energy contribution from the hydrophobic transfer process.[36,37] Lacking corresponding thermodynamic and structural data, an alternative estimate for the hydrophobic contribution to the free energy of binding may be gained by *n*-octanol/water partition coefficients log*P*. Indeed, a prediction of log*P* for hybrids **1** and **2** give values of 2.88 and 4.42, respectively, indicating a more hydrophobic benzimidazole hybrid **2** in line with larger hydrophobic effects and a more favourable binding entropy. It should be noted, however, that the dielectric constant for octanol is 10.3 and with an estimated value of 20 for the DNA minor groove,[39] assessments based on the water-to-octanol partition coefficient are qualitative at best.

4. Conclusions

PBD hybrid molecules constitute a promising type of DNA binding agent. Through their ability of covalent bond formation with guanine bases, high binding affinities with a remarkable increase in the thermal stability of nucleic acid duplexes are observed. Complex formation is significantly promoted by other attached moieties that also impart additional sequence selectivity. Clearly, specific recognition of more than 6 base pairs is presently limited by the size of the two ligands. However, larger DNA binding ligands with the potential of reading longer sequences often suffer from having low delivery capabilities. Typically, they violate the 'rule of five' with respect to their high molecular weight and their num-

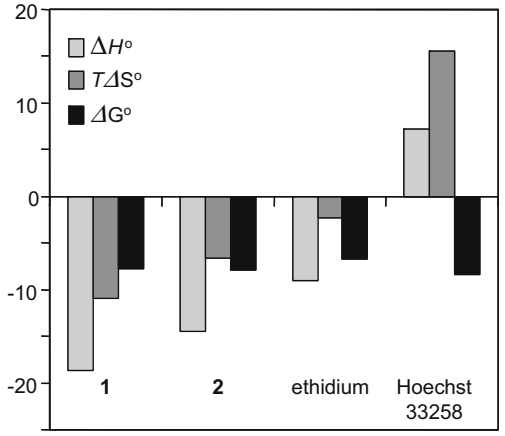

Figure 8. Enthalpic and entropic contributions ΔH° and $T\Delta S^\circ$ to the overall free energy ΔG° as determined by ITC measurements for the interaction with DNA of PBD hybrids **1** and **2** at 20 °C, of the intercalator ethidium at 25 °C[35] and of the minor groove binder Hoechst 33258 at 20.5 °C.[34]

ber of hydrogen bond donors and thus problems may arise in passing through biological membranes to reach the desired nuclear target.

There is ample evidence from the various spectroscopic and calorimetric studies that the structural units attached to the PBD moiety in the two hybrid drugs interact specifically via intercalation in the case of the naphthalimide chromophore and via minor groove binding in the case of the phenyl benzimidazole structure. The analysis of the binding free energy in terms of entropy and enthalpy offers valuable hints for a future rational design of lead compounds with improved binding characteristics. Thus, enthalpy-driven non-covalent binding as observed for the two hybrid drugs suggests that, by introducing suitable substituents, more sequence selectivity can be attained through additional specific hydrogen bonds or electrostatic interactions with the nucleic acid. NMR structural studies on the complexes are in progress and are expected to complement the thermodynamical data, a prerequisite for more specific structural modifications of the drugs.

5. Experimental

5.1. Materials

DNA oligonucleotides were purchased from *TIB MOLBIOL* (Berlin, Germany). Concentrations of the DNA stock solutions were determined spectrophotometrically from absorbances of single-stranded oligonucleotides in distilled water at 80 °C using molar extinction coefficients at 260 nm derived from a nearest-neighbour model.[40] For the measurements, a BPS buffer (20 mM phosphate, 100 mM NaCl, pH 7.0) was used unless otherwise stated.

Naphthalimide-linked PBD hybrids have been prepared by employing vanillin and L-proline methylester as the starting materials. The nitro diethylthioacetal intermediate is coupled with bromo-*N*-alkyl-1,8-naphthalimides followed by reduction of the nitro functionality to give the corresponding amino thioacetal. Deprotection of the amino diethylthioacetal with $HgCl_2$ and HgO affords C-8 linked 1,8-naphthalimide-PBD hybrids.[16] The hybrid ligand **1** with a naphthalimide linked through a piperazine side-armed-alkane spacer to the PBD moiety has been prepared by a similar procedure.[17]

For the synthesis of the benzimidazole-PBD hybrid **2**, 4-[6-(4-methyl-1-piperazinyl)-benzimidazole-2-yl]phenol was used for the coupling with the nitro diethylthioacetal as described.[18]

5.1.1. 7-Methoxy-8-(3-{4-[6-(4-methyl-1-piperazinyl)benzimidazol-2-yl]-phenoxy}propyl)-oxy-(11a*S*)-1,2,3,11a-tetrahydro-5*H*-pyrrolo[2,1-*c*][1,4]benzodiazepin-5-one (2)

A solution of (2*S*)-*N*-{3-(4-[6-(4-methyl-1-piperazinyl)benzimidazol-2-yl]phenoxy]propyl)-oxy-5-methoxy-2-aminobenzoyl} pyrrolidine-2-carboxaldehyde diethyl thioacetal (717 mg, 1 mmol), $HgCl_2$ (613 mg, 2.26 mmol) and $CaCO_3$ (246 mg, 2.46 mmol) in acetonitrile–water (4:1) was slowly stirred at room temperature overnight or until TLC indicated complete loss of starting material. The reaction mixture was diluted with ethyl acetate (30 mL) and filtered through a Celite. The clear yellow organic supernatant was extracted with saturated 5% $NaHCO_3$ (20 mL), brine (20 mL) and the combined organic phase was dried (Na_2SO_4). The organic layer was evaporated in vacuum and purified by column chromatography (80% CH_2Cl_2–MeOH) to give compound **2** (327 mg, 55%). This material was repeatedly evaporated from $CHCl_3$ in vacuum to generate the imine form.

$[\alpha]^{25}_D$ +251.66 (c = 0.5, $CHCl_3$); ^{1}H NMR ($CDCl_3$): δ (ppm) = 1.98 −2.10 (m, 2H), 2.23–2.38 (m, 4H), 2.40 (s, 3H), 2.60–2.75 (m, 4H), 3.10–3.20 (m, 4H), 3.60–3.80 (m, 3H), 3.90 (s, 3H), 4.10–4.30 (m, 4H) 6.79–6.90 (m, 2H), 6.95–7.08 (m, 3H), 7.18–7.42 (d, 2H, J = 8.6 Hz), 7.67–7.65 (d, 1H, J = 4.4 Hz), 7.78–8.10 (d, 2H, J = 9.0 Hz); MS (FAB) 595 $[M+1]^{+\cdot}$.

1-Octanol/water distribution coefficients log$P$ for the hybrids **1** and **2** were predicted using the ALOGPS 2.1 program.

5.2. UV melting experiments

UV experiments were performed on a *Cary 100* spectrophotometer equipped with a Peltier temperature control unit (*Varian* Deutschland, Darmstadt). The melting curves were recorded by measuring the absorption of the solution at 260 nm with 1 data point/°C in 10 mm quartz cuvettes. In general, the UV melting experiments were performed by using a protocol consisting of a first heating cycle, that was followed by cooling the sample to the initial temperature. After a waiting period of ten minutes another heating ramp was started. Heating and cooling rates of 0.5 °C/min were employed. The concentration of the various duplexes was in a range between 3.5 and 6 μM. Drug dissolved in DMSO was added to the DNA solution (total DMSO <4%) in a specific molar ratio (see legend to the figures). Melting temperatures were determined by the maximum of the first derivative plot of the smoothed melting curves.

5.3. Circular dichroism

CD spectra were acquired with a Jasco J-810 spectropolarimeter at 20 °C (*Jasco*, Tokyo, Japan). The spectra were recorded with a bandwidth of 1 nm, a scanning speed of 100 nm/min and 15 accumulations. Concentrations of the drug and the duplex were 6.6 and 3.3 μM for **1** and 10 and 5 μM for **2**, respectively. Both the pure oligonucleotide and the DNA-drug mixture contained an equal percentage of 0.5% DMSO. All spectra were blank corrected.

5.4. Fluorescence measurements

Fluorescence data were recorded with a Jasco FP-6500 spectrofluorometer equipped with a Peltier element and a magnetic stirrer (*Jasco*, Tokyo, Japan). 5 μL aliquots of dissolved hairpin duplex **D2d** were titrated into a cuvette with the drug solution using an automated titrator (Jasco ATS 429). The cuvette of 1 cm path length was initially coated with Sigmacote to prevent drug adsorption on the glass walls. After each addition the solution was allowed to equilibrate for 3 min prior to each measurement. Because the drugs are only poorly soluble in aqueous buffer, both solutions contained small but equal amounts of DMSO (<0.5%). Excitation and emission

bandwidths were 5 nm each. Fluorescence data were recorded with 10 accumulations using a response time of 2 s and with excitation and emission wavelengths set to 315 and 377 nm for **1** and to 325 and 425 nm for **2**, respectively. Blank titrations without drug were performed by injecting the DNA solution into buffer. Corrected fluorescence intensities were determined by subtracting the blank intensities from those of the DNA/drug titrations. All data were normalized. Resulting binding curves were fit to a simple single-site model using Origin 7. The mathematical description of this model is represented by

$$\frac{F}{[M_0]*f_0} = \frac{F_{ML}*K_a*[L]+1}{K_a*[L]+1} \quad (1)$$

$$[L]^2 + \left([M_0] - [L_0] + \frac{1}{K_a}\right)*[L] - \frac{[L_0]}{K_a} = 0 \quad (2)$$

where F is the fluorescence intensity at each titration point, $[M_0]$ and $[L]$ is the total concentration of the drug and the concentration of unbound DNA, respectively, F_{ML} is the fluorescence enhancement factor, f_0 the molar fluorescence of the drug and K_a the binding constant. Solving the quadratic Eq. (2) with the total DNA concentration $[L_0]$ gives the free DNA concentration $[L]$.[24]

5.5. Isothermal titration calorimetry

Experiments were carried out at 20 °C using a MicroCal ITC calorimeter. Three independent measurements were performed starting with different concentrations of the reactants. Typically, 1.8 mL of ligand (4–22 μM) was titrated with a solution of hairpin **D2d** in BPS buffer (100–423 μM). Due to the poor solubility of the drug, 2% of DMSO was added to both the drug and the DNA solution. Injections of 8 μl each were performed with a 290 μL syringe rotating at 307 r.p.m. The smaller first injection step (3 μl) was rejected. The injection time was 16 s and the delay between injections was 4 min. The peaks produced during titration were converted to heat output per injection by integration and correction for the cell volume and sample concentration. Heat of dilution corrections were obtained through injections of oligonucleotide into buffer containing 2% DMSO. The heats produced by the dilution of the PBD-hybrid in buffer were small and therefore neglected. Binding enthalpy ΔH° and the binding constant K_a were obtained by fitting the corrected data to a model with a single binding site. The Origin 7 software (MicroCal) was used for data acquisition and analysis.

References and notes

1. Hurley, L. H.; Petrusek, R. L. *Nature* **1979**, *282*, 529–531.
2. Petrusek, R. L.; Anderson, G. L.; Garner, T. F.; Fannin, Q. L.; Kaplan, D. J.; Zimmer, S. G.; Hurley, L. H. *Biochemistry* **1981**, *20*, 1111–1119.
3. Graves, D. E.; Pattaroni, C.; Krishnan, B. S.; Ostrander, J. M.; Hurley, L. H.; Krugh, T. R. *J. Biol. Chem.* **1984**, *259*, 8202–8209.
4. Waring, M. J.; González, A.; Jiménez, A.; Vázquez, D. *Nucleic Acids Res.* **1979**, *7*, 217–230.
5. Yen, S. F.; Gabbay, E. J.; Wilson, W. D. *Biochemistry* **1982**, *21*, 2070–2076.
6. Harshman, K. D.; Dervan, P. B. *Nucleic Acids Res.* **1985**, *13*, 4825–4835.
7. Embrey, K. J.; Searle, M. S.; Craik, D. J. *Eur. J. Biochem.* **1993**, *211*, 437–447.
8. Bose, D. S.; Thompson, A. S.; Ching, J.; Hartley, J. A.; Berardini, M. D.; Jenkins, T. C.; Neidle, S.; Hurley, L. H.; Thurston, D. E. *J. Am. Chem. Soc.* **1992**, *114*, 4939–4941.
9. Gregson, S. J.; Howard, P. W.; Thurston, D. E.; Jenkins, T. C.; Kelland, L. R. *Chem. Commun.* **1999**, *9*, 797–798.
10. Bailly, C.; Carrasco, C.; Joubert, A.; Bal, C.; Wattez, N.; Hildebrand, M.-P.; Lansiaux, A.; Colson, P.; Houssier, C.; Cacho, M.; Ramos, A.; Braña, M. F. *Biochemistry* **2003**, *42*, 4136–4150.
11. Joubert, A.; Sun, X.-W.; Johansson, E.; Bailly, C.; Mann, J.; Neidle, S. *Biochemistry* **2003**, *42*, 5984–5992.
12. Dervan, P. B. *Science* **1986**, *232*, 464–471.
13. Geierstanger, B. H.; Mrksich, M.; Dervan, P. B.; Wemmer, D. E. *Science* **1994**, *266*, 646–650.
14. David-Cordonnier, M.-H.; Hildebrand, M.-P.; Baldeyrou, B.; Lansiaux, A.; Keuser, C.; Benzschawel, K.; Lemster, T.; Pindur, U. *Eur. J. Med. Chem.* **2007**, *42*, 752–771.
15. (a) Baraldi, P. G.; Cacciari, B.; Guiotto, A.; Leoni, A.; Romagnoli, R.; Spalluto, G.; Mongelli, N.; Howard, P. W.; Thurston, D. E.; Bianchi, N.; Gambari, R. *Bioorg. Med. Chem. Lett.* **1998**, *8*, 3019–3024; (b) Kamal, A.; Rao, M. V.; Laxman, N.; Ramesh, G.; Reddy, G. S. K. *Curr. Med. Chem.—Anti-Cancer Agents* **2002**, *2*, 215–254; (c) Kumar, R.; Lown, J. W. *Oncol. Res.* **2003**, *13*, 221–233; (d) Wells, G.; Martin, C. R. H.; Howard, P. W.; Sands, Z. A.; Laughton, C. A.; Tiberghien, A.; Woo, C. K.; Masterson, L. A.; Stephenson, M. J.; Hartley, J. A.; Jenkins, T. C.; Shnyder, S. D.; Loadman, P. M.; Waring, M. J.; Thurston, D. E. *J. Med. Chem.* **2006**, *49*, 5442–5461.
16. Kamal, A.; Reddy, B. S. N.; Reddy, G. S. K.; Ramesh, G. *Bioorg. Med. Chem. Lett.* **2002**, *12*, 1933–1935.
17. (a) Kamal, A.; Ramu, R.; Khanna, G. B. R. US Patent 6,979,684 (27.12.05); PCT/IN04/00191 (30.06.04).; (b) Ramu, R. Ph.D thesis, Kakatiya University, Warangal (India), **2005**.; (c) Kamal, A.; Ramu, R.; Tekumalla, V.; Khanna, G. B. R.; Barkume, M. S.; Juvekar, A. S.; Zingde, S. M. *Bioorg. Med. Chem.* **2008**, *16*, 7218–7224.
18. Kamal, A.; Ramulu, P.; Srinivas, O.; Ramesh, G.; Kumar, P. P. *Bioorg. Med. Chem. Lett.* **2004**, *14*, 4791–4794.
19. Bostock-Smith, C. E.; Searle, M. S. *Nucleic Acids Res.* **1999**, *27*, 1619–1624.
20. Kamal, A.; Reddy, P. S. M. M.; Reddy, D. R.; Laxman, E. *Bioorg. Med. Chem.* **2006**, *14*, 385–394.
21. Kizu, R.; Draves, P. H.; Hurley, L. H. *Biochemistry* **1993**, *32*, 8712–8722.
22. Narayanaswamya, M.; Griffiths, W. J.; Howard, P. W.; Thurston, D. E. *Anal. Biochem.* **2008**, *374*, 173–181.
23. Rogers, J. E.; Weiss, S. J.; Kelly, L. A. *J. Am. Chem. Soc.* **2000**, *122*, 427–436.
24. Eftink, M. R. *Methods Enzymol.* **1997**, *278*, 221–257.
25. Kohn, K. W.; Spears, C. L. *J. Mol. Biol.* **1970**, *51*, 551–572.
26. Hurley, L. H.; Gairola, C.; Zmijewski, M. *Biochem. Biophys. Acta* **1977**, *475*, 521–535.
27. Hurley, L. H.; Allen, C. S.; Feola, J. M.; Lubawy, W. C. *Cancer Res.* **1979**, *39*, 3134–3140.
28. Tanious, F. A.; Yen, S.-F.; Wilson, W. D. *Biochemistry* **1991**, *30*, 1813–1819.
29. Zakrzewska, K.; Pullman, B. *J. Biomol. Struct. Dynamics* **1986**, *4*, 127–136.
30. Schipper, P. E.; Nordén, B.; Tjerneld, F. *Chem. Phys. Lett.* **1980**, *70*, 17–21.
31. Nordén, B.; Kurucsev, T. *J. Mol. Recognit.* **1994**, *7*, 141–156.
32. Rosu, F.; Gabelica, V.; Houssier, C.; De Pauw, E. *Nucleic Acids Res.* **2002**, *30*, e82.
33. Han, F.; Taulier, N.; Chalikian, T. V. *Biochemistry* **2005**, *44*, 9785–9794.
34. Haq, I.; Ladbury, J. E.; Chowdhry, B. Z.; Jenkins, T. C.; Chaires, J. B. *J. Mol. Biol.* **1997**, *271*, 244–257.
35. Ren, J.; Jenkins, T. C.; Chaires, J. B. *Biochemistry* **2000**, *39*, 8439–8447.
36. Chaires, J. B. *Biopolymers* **1998**, *44*, 201–215.
37. Haq, I. *Arch. Biochem. Biophys.* **2002**, *403*, 1–15.
38. Chaires, J. B. *Arch. Biochem. Biophys.* **2006**, *453*, 26–31.
39. Jin, R.; Breslauer, K. J. *Proc. Natl. Acad. Sci. USA* **1988**, *85*, 8939–8942.
40. Watkins, N. E., Jr.; SantaLucia, J., Jr. *Nucleic Acids Res.* **2005**, *33*, 6258–6267.